Mapping the Integrin $\alpha_V\beta_3$−Ligand Interface by Photoaffinity Cross-Linking[†]

Gal Bitan, Lukas Scheibler, Zvi Greenberg, Michael Rosenblatt, and Michael Chorev*

Division of Bone and Mineral Metabolism, Charles A. Dana and Thorndike Laboratories, Department of Medicine, Beth Israel Deaconess Medical Center and Harvard Medical School, 330 Brookline Avenue, Boston, Massachusetts 02215

Received August 12, 1998; Revised Manuscript Received January 19, 1999

ABSTRACT: Integrins are cell surface adhesion molecules involved in mediating cell−extracellular matrix interactions. High-resolution structural data are not available for these heterodimeric receptors. Previous cross-linking studies of integrins aimed at elucidating the nature of the receptor−ligand interface have been limited to identification of relatively large binding domains. To create reagents for "photoaffinity scanning" of the RGD-binding site of human integrin $\alpha_V\beta_3$, new conformationally constrained ligands were designed. These photoreactive ligands are based on cyclo Ac-[Cys-Asn-Dmt-Arg-Gly-Asp-Cys]-OH, which displays an affinity of 50 nM for $\alpha_V\beta_3$. This molecular scaffold was modified at the C-terminus by a benzophenone-containing amino acid residue, L-4-benzoylphenylalanine (Bpa). At the N-terminus, a molecular tag was introduced in the form of radioactive iodine or biotin. The newly designed tagged photoreactive RGD-containing ligands display an affinity of 0.5−0.7 μM for $\alpha_V\beta_3$, and cross-link efficiently and specifically to the receptor. A 100 kDa band corresponding to the β_3 subunit−ligand conjugate was detected as the major cross-linking product. Cross-linking was dependent upon the presence of Ca^{2+} and Mg^{2+} ions, and was competitively inhibited by a nonphotoreactive ligand. Enzymatic and chemical digestions of the radiolabeled photoconjugate enabled identification of a 20-amino acid fragment between positions 99 and 118 in the β_3 chain of the integrin as the contact domain for ligand at a site adjacent to the C-terminal portion of the RGD triad.

Integrins are membrane-bound cell surface adhesion molecules involved in cell−extracellular matrix (ECM)[1] and cell−cell interactions (*1, 2*). These receptors are composed of two subunits, α and β, both characterized by a large N-terminal extracellular component, a transmembrane domain, and a short C-terminal intracellular tail. Currently, there are 23 known combinations between the 17 α and eight β subunits. These heterodimers are presented on diverse cell types across many tissues (*3*).

The current model of the integrin molecule is complex. Both the α and the β subunits are required for generating a functional receptor, and binding of divalent metal cations such as Ca^{2+} and Mg^{2+} is essential for ligand recognition. These interactions have been the subject of numerous investigations (*2, 3*). Repetitive metal-binding motifs (termed EF-hand-like or MIDAS domains) have been identified in the N-terminal part of β subunits and in the inserted I domain of some α subunits. Utilization of ligand-induced binding site (LIBS) antibodies as well as other methods provides evidence of close proximity between metal- and ligand-

binding sites (*3−5*). However, the nature of the actual interaction among an integrin, its ligand, and divalent metal cations remains to be elucidated.

The most common integrin binding sequence is the arginyl-glycyl-aspartyl (RGD) motif, found within many ECM proteins and disintegrins (*6*). Selectivity for different RGD-containing ligands by different integrins is attributed to the sequences flanking the RGD triad, the conformational presentation of the triad, and auxiliary binding motifs in the ligand (*7−9*).

Of special interest is the $\alpha_V\beta_3$ integrin (vitronectin receptor), which binds various RGD-containing proteins, including fibronectin, fibrinogen, vitronectin, von Willebrand factor, bone sialoprotein, and osteopontin, as well as many disintegrins and small RGD-containing peptides. It plays a role in numerous physiological processes such as angiogenesis, apoptosis, and bone resorption. $\alpha_V\beta_3$ is the most abundant integrin on osteoclasts, the multinucleated cells responsible for bone resorption. Interaction between $\alpha_V\beta_3$ and the bone matrix may serve to form the intimate cell−matrix "tight seal" essential for the resorptive process (*10*). Therefore, inhibition of $\alpha_V\beta_3$ function may provide a novel mechanism-based approach for treatment of diseases associated with increased bone resorption such as osteoporosis (*11, 12*).

Rational design of antagonists of integrin receptors should benefit from a detailed understanding of the structure of the integrin−ligand complex. Due to their large size and because they are membrane-bound, integrins have not been amenable to high-resolution structural characterization by X-ray crystallography or NMR. Nevertheless, structure−function in-

¹ Abbreviations: Ahx, 6-aminohexanoyl; BH, Bolton-Hunter reagent; Bpa, L-4-benzoylphenylalanine; BSA, bovine serum albumin; Dmt, L-5,5-dimethylthiazolidinecarboxylic acid; ECM, extracellular matrix; Endo-F, endoglycosidase-F/*N*-glycosidase-F; LIBS, ligand-induced binding site; Lys-C, lysyl endopeptidase; NHS, *N*-hydroxysuccinimide; PTH, parathyroid hormone; TBS, Tris-buffered saline.
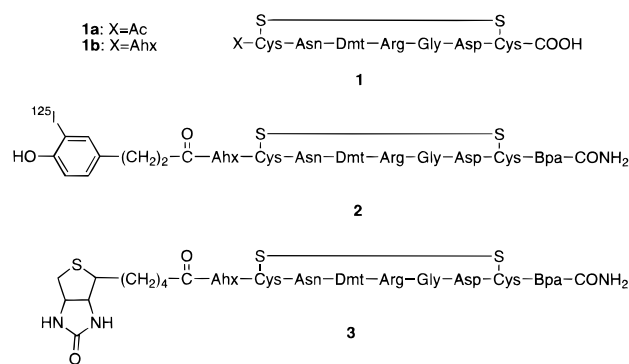
FIGURE 1: Schematic formulas of cyclic scaffold **1** and its tagged photoreactive analogue **2**.

formation has been generated by indirect methods such as mutational analysis (*13−15*), creation of receptor chimeras (*16−18*) and deletions (*19*) by recombinant techniques, biological characterization of peptides derived from putative binding sites (*20*), and generation of activating (*5*) or inhibitory antibodies (*20, 21*).

Most of these approaches focus exclusively on either the ligand or the integrin receptor. Hence, the information obtained about the nature of the bimolecular interaction is indirect or inferred. The advantage of the cross-linking methodology, used in this work, is that it offers a direct approach to identifying interacting sites between receptor and ligand. Studies in which interface is scanned by individually cross-linking several different ligands to a receptor could eventually be used to generate an experimentally-based structure of the receptor−ligand complex (*22*).

Early attempts to elucidate the nature of the bimolecular interaction between β_3-containing integrins, such as $\alpha_V\beta_3$ and $\alpha_{IIb}\beta_3$, and radioiodinated RGD-containing ligands employed either homobifunctional chemical cross-linkers (*23*) or aryl azide-based photoaffinity agents (*24, 25*). The predominant cross-linking occurred with the β_3 subunit and identified only large segments within the receptor, such as the sequences of residues 109−171 (*23*) and 217−302 (*25*) in $\alpha_{IIb}\beta_3$ or 61−203 (*24*) in $\alpha_V\beta_3$. More recently, a cross-linking study with integrin $\alpha_4\beta_1$ identified a small domain in β_1 (*26*), which contains a putative cation binding motif. A homologous motif is found in the regions identified by cross-linking studies with the β_3 subunit (*23, 24*).

Recently, benzophenone-based "photoaffinity scanning" has emerged as the method of choice for mapping interfaces of ligand−receptor complexes (*27−33*). The advantageous properties of the benzophenone moiety include low reactivity with water, favorable photokinetics with high cross-linking specificity and efficiency, and convenience in synthesis, purification, and handling (*34−36*). These properties were exploited in recent years for probing the interaction between substrates and the enzyme steroid 5α-reductase (*27*) and other bimolecular interactions, such as those which involve a ligand molecule and the neurokinin-1 receptor (*28, 29*), the parathyroid hormone (PTH)/PTH-related protein receptor (*22, 30, 31*), the urokinase-type plasminogen activator receptor (*32*), and the angiotensin AT$_4$ receptor (*33*).

To map the interface of the human $\alpha_V\beta_3$−ligand complex, we developed biologically active RGD-based ligands which contain a benzophenone moiety positioned at the C-terminus adjacent to the RGD pharmacophore. The design, synthesis,

and characterization of these and other ligands will be described elsewhere. Here, we used a high-affinity conformationally constrained RGD-containing ligand, cyclo Ac-[Cys-Asn-Dmt-Arg-Gly-Asp-Cys]-OH (**1a**, IC$_{50}$ = 50 nM) (*37*), as a molecular scaffold for carrying the requisite components for photoaffinity cross-linking. This scaffold was extended at the C-terminus by the photoreactive residue L-4-benzoylphenylalanine (Bpa). A molecular tag, either the [^{125}I]-Bolton-Hunter (BH) moiety (in analogue **2**) or the biotin moiety (in analogue **3**), was introduced at the N-terminus through a 6-aminohexanoyl (Ahx) spacer (Figure 1). Both the radioiodinated and the biotinylated analogues display a high affinity for and cross-link efficiently to $\alpha_V\beta_3$. The radiolabeled photoreactive ligand **2** allowed us to identify a first contact domain between the integrin $\alpha_V\beta_3$ and the Bpa residue, located two amino acids C-terminal to the RGD motif.

EXPERIMENTAL PROCEDURES

Purification of Human Integrin $\alpha_V\beta_3$. Recombinant human integrin $\alpha_V\beta_3$ stably expressed in high levels in HEK 293 cells was purified using a monoclonal antibody (LM609) affinity column (*37*).

Radioreceptor Binding Assay. The affinity of the peptides for purified integrin $\alpha_V\beta_3$ was measured in a radioreceptor binding assay by competition with [^{125}I]echistatin (*37*).

Introduction of [^{125}I]Bolton-Hunter. Thirty three micrograms (16 nmol) of peptide **1b** dissolved in 100 μL of 0.1 M sodium phosphate buffer (pH 8.0) was incubated with 1 mCi of [^{125}I]Bolton-Hunter reagent at 0 °C for 2 h and then at room temperature overnight. The mixture was purified on a RP-HPLC Nova-Pak C18 column (3.9 mm × 150 mm) (Waters, Milford, MA) with a solvent system of A (0.1% TFA in H$_2$O) and B (0.1% TFA in ACN). The purification was carried out using a linear gradient of 22 to 38% B in A, for 30 min at a flow rate of 1 mL/min, monitored at 220 nm. The radioactive peak was collected (0.5 min/fraction), and the radioactivity in each fraction was monitored by a γ-radiation counter. The fractions containing the radioactive peak were pooled and stored at −80 °C.

Photoaffinity Cross-Linking to Purified $\alpha_V\beta_3$. Experiments were performed in 24- or 6-well plastic plates (Costar, Cambridge, MA). The plate was blocked for 1 h with Tris-buffered saline (TBS) [150 mM NaCl and 25 mM Tris-HCl (pH 7.5)] containing 1% bovine serum albumin (BSA) and then washed five times with TBS. Purified $\alpha_V\beta_3$ (0.1 nmol) in TBS supplemented with 1 mM CaCl$_2$ and 1 mM MgCl$_2$, photoreactive peptide **2** or **3**, and in appropriate cases the nonphotoreactive peptide **1a** as a competitor were diluted to a final volume of 250 μL (24-well plate) or 1.5 mL (6-well plate) and incubated for 1 h at room temperature. The ligand was used at 10^6 cpm (≈0.2 pmol) per reaction. The mixtures were irradiated with 365 nm UV light for 1 h at 4 °C in a Stratalinker 2400 cross-linker (Stratagen, La Jolla, CA) and were then subjected to SDS−PAGE analysis. The photoconjugates of ^{125}I-labeled peptide **2** and receptor were visualized by autoradiography. The photoconjugates of the biotin-labeled peptide **3** and receptor were visualized by Western blotting using a streptavidin amplified alkaline phosphatase Immun-Blot kit (Bio-Rad, Hercules, CA) or the avidin−horseradish peroxidase conjugate.
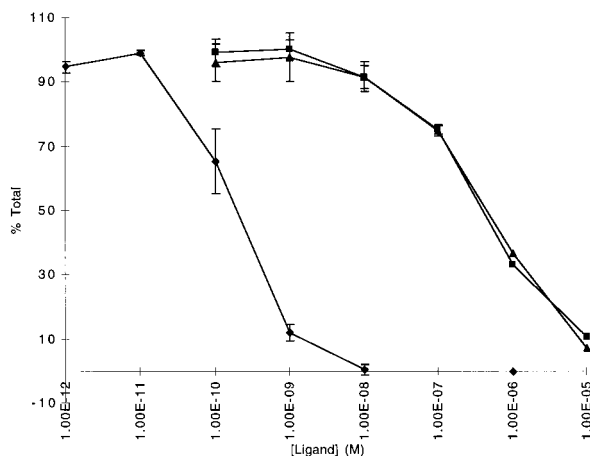
FIGURE 2: Binding curves of nonradioactive peptide **2** and echistatin as a positive control. [^{125}I]Echistatin was used as a tracer: echistatin (◆), peptide **2** (■), and peptide **3** (▲).

Photoaffinity Cross-Linking to HEK 293 Cells Stably Expressing Integrin $\alpha_V\beta_3$ at High Levels. Experiments were performed using harvested cells from ten 75 cm^2 plates at confluency resuspended into a 6-well plate (2 mL per well) and 4×10^7 cpm of ^{125}I-labeled peptide **2** as described previously (*30*). Following cross-linking, the cells were washed and lysed by five freeze−thaw cycles, and the ligand−receptor photoconjugate was extracted and purified by preparative SDS−PAGE after reduction and alkylation of Cys residues by iodoacetamide (*30*).

Enzymatic and Chemical Cleavage. Digestions of the β_3−**2** photoconjugate by endoglycosidase-F/*N*-glycosidase-F (Endo-F), lysyl endopeptidase (Lys-C), and cyanogen bromide (CNBr) were performed as previously described (*30*).

RESULTS

Photoaffinity Cross-Linking. The nonradioactive form of iodinated peptide **2** and the biotinylated peptide **3** were evaluated for their binding affinity toward $\alpha_V\beta_3$ by a radioreceptor binding assay using [^{125}I]echistatin as a tracer (Figure 2). Although a 25−35-fold decrease in affinity relative to **1a** was revealed, the IC$_{50}$ values found for **2** and **3** (0.7 ± 0.4 and 0.5 ± 0.05 μM, respectively) were sufficient for efficient and highly specific cross-linking. Analogues **2** and **3** were cross-linked to the integrin $\alpha_V\beta_3$ by UV light irradiation. The photoconjugates obtained with **2** and **3** were analyzed by SDS−PAGE/autoradiography or SDS−PAGE/ Western blot, respectively. Figure 3 shows the cross-linking of **3** to purified $\alpha_V\beta_3$ and of **2** to either purified integrin or to integrin displayed on intact HEK 293 cells. There is a clear predominance of cross-linking to the β_3 chain. The β/α ratio assessed by densitometry or by comparing the radioactivity of purified **2**−β_3 and **2**−α_V conjugates generated in the same experiment is 97 ± 1:3 ± 1 for both cross-linking modes. As shown in Figure 3C, cross-linking is competed in a dose-dependent manner by addition of **1a**. No cross-linking is observed in the presence of 4 mM EDTA. Thus, the cross-linking is specific and dependent on the presence of Ca^{2+} and Mg^{2+} ions. Similar results were observed for peptide **3** (not shown).

*Identification of the Binding Domain in Integrin $\alpha_V\beta_3$ for Peptide **2***. Attempts to identify the contact domain by analyzing the photoconjugate generated by cross-linking
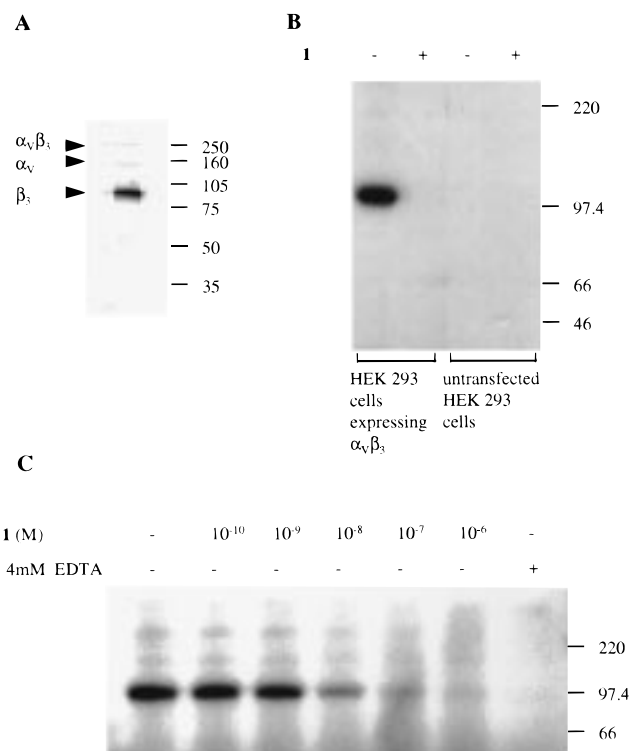

FIGURE 3: Cross-linking of analogues **2** and **3** to $\alpha_V\beta_3$. (A) Cross-linking of analogue **3** to purified soluble $\alpha_V\beta_3$. The major band revealed by 7.5% acrylamide SDS−PAGE/Western blot analysis (developed with amplified alkaline phosphatase) corresponds to the β_3 subunit. Only a minor band generated by cross-linking to α_V is observed. The faint band at 250 kDa corresponds to the $\alpha_V\beta_3$ heterodimer and is the result of incomplete denaturation prior to electrophoresis. (B) Cross-linking of analogue **2** to HEK 293 cells stably expressing a high level of $\alpha_V\beta_3$ integrin vs wild-type HEK 293 cells with and without competition with 10^{-5} M peptide **1a**. Samples were analyzed by 7.5% acrylamide SDS−PAGE/autoradiography. (C) Inhibition of cross-linking of purified soluble $\alpha_V\beta_3$ to analogue **2** by competition with peptide **1a** or by addition of EDTA. Samples were analyzed by 7.5% acrylamide SDS−PAGE/ autoradiography.

peptide **2** to the purified integrin failed due to rapid autoradiolysis. A different problem was encountered using peptide **3**. Although the β_3−**3** photoconjugate was readily detected by Western blot, the amounts generated after digestion of the photoconjugate with the different cleavage agents were insufficient to allow reliable (color or chemiluminescence) detection by amplified avidin−alkaline phosphatase. Therefore, we decided to cross-link the radioactive ligand **2** to the recombinant integrin receptor presented on intact HEK 293 cells. The amount of nonspecific cross-linking was similar to that obtained with the soluble purified receptor (Figure 3), but rapid autoradiolysis was not observed.

Chemical digestion of the β_3−**2** photoconjugate with CNBr, which cleaves selectively at the carboxyl side of Met residues, yields a major radioactive band with an apparent molecular mass of 15−16 kDa as determined by SDS−PAGE analysis (Figure 4). Analysis of the theoretical CNBr digestion map of the mature β_3 chain identifies a 95-amino acid fragment, β_3[24−118], which is glycosylated at position 99, as a potential contact domain. The calculated mass of this conjugated fragment, assuming the carbohydrate moiety adds 3 kDa (*26*), is 15.3 kDa, which is consistent with the size of the experimentally generated band after CNBr
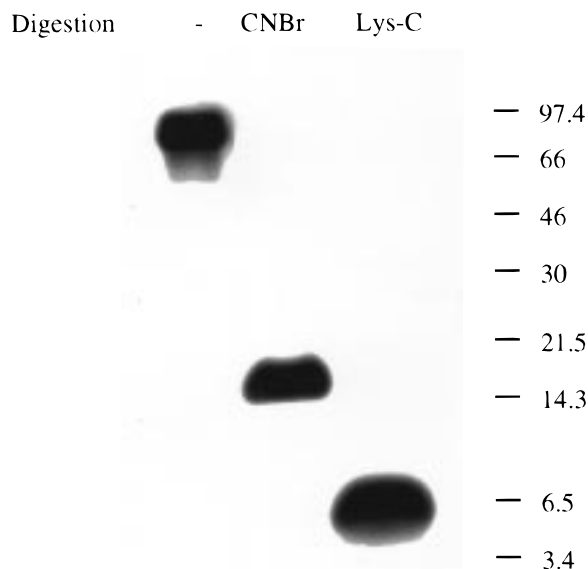
Digestion — CNBr Lys-C

— 97.4

— 66

— 46

— 30

— 21.5

— 14.3

— 6.5

— 3.4

FIGURE 4: Primary cleavage pattern of the β$_3$−**2** conjugate by CNBr and Lys-C. The digestion products were analyzed by 16.5% SDS−PAGE (Tricine buffer system)/autoradiography. Molecular masses of prestained markers are indicated on the right.

treatment. Deglycosylation of the CNBr-generated band with Endo-F produces the expected ≈3 kDa decrease in molecular mass (Figure 5A). On the basis of analysis of the DNA-derived amino acid sequence of the human β$_3$ chain (*38*), no other fragment with this mass can be generated by CNBr cleavage.

   Enzymatic digestion with Lys-C, which cleaves selectively on the C-terminal side of Lys residues, yields a single radiolabeled band corresponding to ≈7 kDa (Figure 4). The putative Lys-C-generated ligand−β$_3$ conjugated fragments that overlap with the putative CNBr-generated ligand−β$_3$-[24−118] conjugated fragment may correspond to one of the following sequences: residues 1−41, 47−72, 73−98, and 99−125 (which is glycosylated), for which the calculated molecular masses are 4.3, 2.9, 2.8, and 6.3 kDa, respectively (Figure 6). Combined with the molecular mass of the ligand (1.5 kDa), these fragments would generate radioactive bands in the molecular mass range of 5.3−7.8 kDa which, due to the limited level of resolution of the SDS−PAGE analysis, cannot be unambiguously assigned. Secondary digestion of the 7 kDa Lys-C-derived band with Endo-F generated a new radiolabeled band ≈4 kDa in size (Figure 5B). Therefore, of the four potential Lys-C-generated ligand−β$_3$ conjugate fragments, we can now assign β$_3$[99−125], the only glyco-sylated fragment, as the putative site of cross-linking. To further validate this conclusion, we carried out a set of two reciprocal secondary digestions which linked between the two independent digestion pathways. The CNBr-generated fragment was digested with Lys-C, and the Lys-C-generated fragment was digested by CNBr. As shown in Figure 5C, Lys-C treatment of the CNBr-generated fragment β$_3$[24−118] produced the expected reduction of approximately 10 kDa in molecular mass and yielded fragment β$_3$[99−118]. The original Lys-C-generated fragment β$_3$[99−125] is only reduced by seven amino acids upon CNBr digestion. The difference between the original fragment β$_3$[99−125] and the product of the secondary digestion β$_3$[99−118] is not distinguishable in the resolution provided by the SDS−PAGE analysis (Figure 5C).

A

CNBr + +
Endo-F - +

220 —
97.4 —
66 —
46 —
30 —
21.5 —
14.3 —
6.5 —

B

Lys-C - + + +
Endo-F + + - +

97.4 —
66 —
46 —
30 —
21.5 —
14.3 —
6.5 —
3.4 —

C

Lys-C + + - +
CNBr - + + +

97.4 —
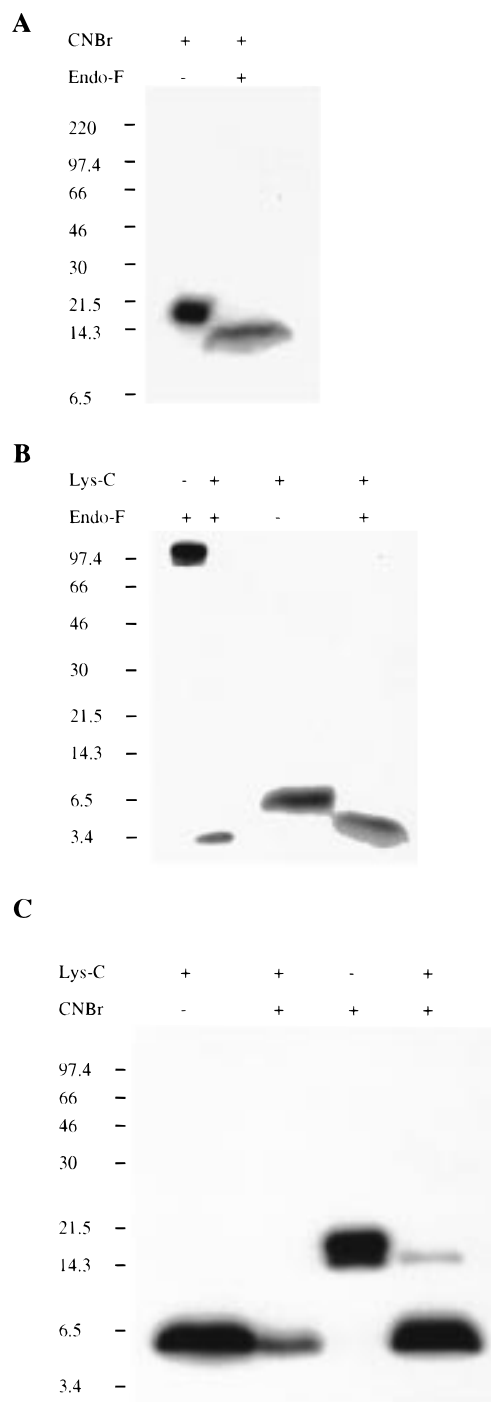66 —
46 —
30 —
21.5 —
14.3 —
6.5 —
3.4 —

FIGURE 5: Secondary digestions. (A) Deglycosylation of the CNBr-generated fragment reveals the expected decrease in molecular mass (10 to 20% gradient gel, Tricine buffer system). (B) Deglycosylation of the Lys-C-generated fragment or Lys-C digestion of the deglycosylated β$_3$−**2** conjugate yields the same product, validating that the original Lys-C-generated fragment is the glycosylated sequence β$_3$[99−125] (10 to 20% gradient gel, Tricine buffer system). (C) Reciprocal secondary digestions of the two independent pathways. From left to right, Lys-C digestion of the β$_3$−**2** conjugate, CNBr digestion of the Lys-C-generated fragment, CNBr digestion of the β$_3$−**2** conjugate, and Lys-C digestion of the CNBr-generated fragment. The residual upper band in the right lane represents incomplete digestion of the CNBr; the fragments in the second and fourth lanes correspond to the minimal cleavage-restricted domain β$_3$[99−118] (16.5% Tricine gel).

   We conclude that the 20-amino acid sequence N[99]-FSIQVRQVEDYPVDIYYLM[118] of the β$_3$ chain represents
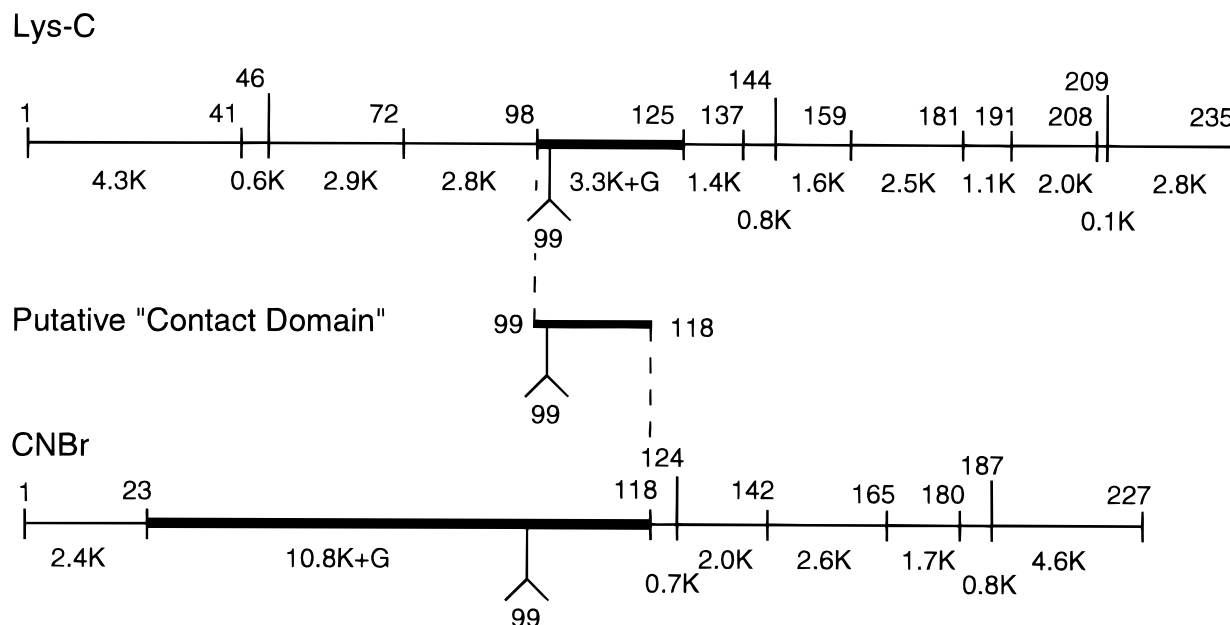
FIGURE 6: Predicted digestion map of the region of residues 1−235 of the β_3 chain. Cleavage points are shown for Lys-C and for the Met-specific reagent CNBr. The domains identified in the cleavage paths used (see the text and the legends of Figures 4 and 5) are highlighted in bold lines. The inverted Y represents a glycosylation site.

a minimal cleavage restricted domain which includes the contact site between β_3 and photoligand **2** (Figure 6). This contact domain is generated by the restriction sites at K[98] and M[118] which are the boundaries of the relevant Lys-C and CNBr cleavages, respectively.

DISCUSSION

We have undertaken an effort to use recent advances in photoaffinity cross-linking methodology as a means of elucidating directly the contact site within the $\alpha_V\beta_3$ integrin for an RGD-containing ligand. In contrast to previous cross-linking studies in the integrin field, our objective goes beyond identifying a large binding domain. Rather, our efforts are directed at generating a detailed map of the ligand−receptor interface. Obviously, only an ensemble of contact sites, the first of which is presented in this work, will lead to the characterization of the topology of the intermolecular surface.

Cross-linking with ligands **2** and **3** appears to be highly specific, as evidenced by the absolute requirement for the presence of divalent metal cations, and by the dose-dependent competition with the unmodified peptide **1a**. Exploration of the specificity of the photoreactive ligands for $\alpha_V\beta_3$ versus those for other integrins is outside the scope of this work.

The short half-life of ^{125}I represents a potential disadvantage. Analysis needs to be performed expeditiously, and repeated preparation of the photoreactive radioligand is required. However, the 1000-fold higher sensitivity of detection of the radioactive as compared to the biotin tag greatly facilitates the monitoring of purification of the photoconjugated fragments. In addition, these procedures are encumbered by the special handling requirements of radioactivity. Despite these potential disadvantages, the overriding issue with use of a biotin tag is the inferior sensitivity of biotin detection. This is true despite the use of the amplified alkaline phosphatase system.

Benzophenone cross-linking to either purified $\alpha_V\beta_3$ or the intact integrin receptor expressed on the membrane surface

of HEK 293 cells yields highly pure and uniformly labeled β_3 subunit. Only minor amounts of α_V chain and, in the cell-bound receptor, negligible impurities originating from very low levels of endogenously expressed integrins (different from $\alpha_V\beta_3$) are photolabeled. The chemical and enzymatic digestions were performed on the β_3-**2** photoconjugate following a one-step purification of the conjugate by preparative SDS−PAGE. By carefully comparing the experimental data generated using the two independent digestion paths with the putative cleavage map for each cleavage agent, and by validating these pathways through reciprocal and complementing secondary digestions, we delineate unambiguously the contact site between peptide **2** and the integrin $\alpha_V\beta_3$ as the 20-mer peptide corresponding to residues 99−118 of the β_3 chain.

This result is in agreement with the previously identified fragment (residues 61−203), obtained in a cross-linking study conducted a decade ago (*24*), using a relatively low-resolution system. The current study relies on a more advanced methodology in which the results are validated by two independent digestion pathways, and the size of the identified domain is further delineated from 143 (*24*) to 20 amino acids.

Most of the relevant structural data in this field have been obtained for integrins related to $\alpha_V\beta_3$, such as the platelet fibrinogen receptor $\alpha_{IIb}\beta_3$ (*39*). These studies identified sequences crucial for metal coordination and ligand binding. Analogous domains could have similar roles in $\alpha_V\beta_3$. The contact domain in $\alpha_V\beta_3$ found in this work has not been previously reported. It is adjacent to residues 118−131, a region considered to be crucial for ligand binding in $\alpha_{IIb}\beta_3$ (*20*). This domain was identified by binding of an activation-dependent monoclonal antibody (mAb) and by inhibition of fibrinogen binding by the corresponding peptide, β_3[118−131]. Within this sequence, residues 119−123 form a DXSXS motif which is postulated to be a metal binding motif (*13−15*). In the vicinity of residues 118−131 in the β_3 chain

(in $\alpha_{IIb}\beta_3$), the sequences of residues 101−109 and 109−128 are binding epitopes of activation-dependent mAbs P$_2$37 and AC7, respectively (*40, 41*). Molecular modeling and mutational analysis of $\alpha_{IIb}\beta_3$ identified oxygen-containing residues located further toward the C-terminus which appear to be important for binding (*15*). Integrin chimera studies revealing regions which confer ligand specificity (*17, 18*) and antibody binding studies using ligand-induced binding site (LIBS) antibody AP5, which has been shown to be an activating antibody in both $\alpha_{IIb}\beta_3$ and $\alpha_V\beta_3$ (*5*), identify yet additional sites in the β_3 chain which appear to be important for integrin functionality. The encouraging recent report on the efficient expression of a functional soluble form of integrin $\alpha_{IIb}\beta_3$ (*19*) may provide access to a complementary approach for elucidating the structure of the ligand−receptor interface via spectroscopic or crystallographic structural analysis.

While all of the findings described above provide significant information with regard to the participation or influence of certain regions of the β_3 chain in ligand binding, our data provide direct evidence for the first time of a small contact domain in the β_3 chain which interacts directly with the C-terminus of a short RGD-containing peptide. Our data indicate that the region of residues 99−118 is part of the ligand-binding surface of the β_3 chain.

Our system may introduce some bias because of the bulkiness of the benzophenone group and the differential reactivity of the photoactivated intermediate toward different amino acid side chains. However, the close proximity between the benzophenone group and the RGD triad in ligand **2** and the requirement for very close proximity between the benzophenone and the cross-linking site (*34*) suggest that the newly identified contact site participates in, or is very close to, the RGD binding site.

This work represents a first step toward the detailed characterization of the interface between RGD-containing ligands and the $\alpha_V\beta_3$ integrin. The finding that the novel photoreactive analogue **2** can efficiently and specifically cross-link to the integrin receptor and generate a sufficient amount of ligand−β_3 photoconjugate to allow mapping by protein digestion is a demonstration of proof of principle for the photoaffinity cross-linking approach in this system. We now plan to use photoaffinity scanning in a systematic effort to generate a topological map of the binding surfaces between ligand and integrin. The degree of resolution of this map will depend on the number and quality of contact sites identified as additional tagged photoreactive ligands are employed. Of particular utility will be those ligands in which the benzophenone-bearing sites are located in close proximity and at diverse spatial orientations relative to the RGD triad. Such photoligands are now being prepared.

REFERENCES

1. Hynes, R. O. (1992) *Cell 69*, 11−25.
2. Stuiver, I., and O'Toole, T. E. (1995) *Stem Cells (Dayton) 13*, 250−262.
3. Garratt, A. N., and Humphries, M. J. (1995) *Acta Anat. 154*, 34−45.
4. Smith, J. W., and Cheresh, D. A. (1991) *J. Biol. Chem. 266*, 11429−11432.
5. Pelletier, A. J., Kunicki, T., and Quaranta, V. (1996) *J. Biol. Chem. 271*, 1364−1370.
6. Ruoslahti, E. (1996) *Annu. Rev. Cell Dev. Biol. 12*, 697−715.
7. Marcinkiewicz, C., Vijay-Kumar, S., McLane, M. A., and Niewiarowski, S. (1997) *Blood 90*, 1565−1575.
8. Kunicki, T. J., Annis, D. S., and Felding-Habermann, B. (1997) *J. Biol. Chem. 272*, 4103−4107.
9. Abrams, C., Deng, Y. J., Steiner, B., O'Toole, T., and Shattil, S. J. (1994) *J. Biol. Chem. 269*, 18781−18788.
10. Horton, M. A. (1997) *Int. J. Biochem. Cell Biol. 29*, 721−725.
11. Engleman, V. W., Nickols, G. A., Ross, F. P., Horton, M. A., Griggs, D. W., Settle, S. L., Ruminski, P. G., and Teitelbaum, S. L. (1997) *J. Clin. Invest. 99*, 2284−2292.
12. Yamamoto, M., Fisher, J. E., Gentile, M., Seedor, J. G., Leu, C.-T., Rodan, S. B., and Roden, G. A. (1998) *Endocrinology 139*, 1411−1418.
13. Loftus, J. C., O'Toole, T. E., Plow, E. F., Glass, A., Frelinger, A. L., III, and Ginsberg, M. H. (1990) *Science 249*, 915−918.
14. Bajt, M. L., and Loftus, J. C. (1994) *J. Biol. Chem. 269*, 20913−20919.
15. Tozer, E. C., Liddington, R. C., Sutcliffe, M. J., Smeeton, A. H., and Loftus, J. C. (1996) *Cell 79*, 659−667.
16. Loftus, J. C., Halloran, C. E., Ginsberg, M. H., Feigen, L. P., Zablocki, J. A., and Smith, J. W. (1996) *J. Biol. Chem. 271*, 2033−2039.
17. Takagi, J., Kamata, T., Meredith, J., Puzon-McLaughlin, W., and Takada, Y. (1997) *J. Biol. Chem. 272*, 19794−19800.
18. Lin, E. C. K., Ratnikov, B. I., Tsai, P. M., Carron, C. P., Myers, D. M., Barbas, C. F., III, and Smith, J. W. (1997) *J. Biol. Chem. 272*, 23912−23920.
19. Peterson, J. A., Visentin, G. P., Newman, P. J., and Aster, R. H. (1998) *Blood 92*, 2053−2063.
20. D'Souza, S. E., Haas, T. A., Piotrowicz, R. S., Byers-Ward, V., McGrath, D. E., Soule, H. R., Cierniewski, C., Plow, E. F., and Smith, J. W. (1994) *Cell 79*, 659−667.
21. Barbas, C. F., III, Languino, L. R., and Smith, J. W. (1993) *Proc. Natl. Acad. Sci. U.S.A. 90*, 10003−10007.
22. Zhou, A. T., Bessalle, R., Bisello, A., Nakamoto, C., Rosenblatt, M., Suva, L. J., and Chorev, M. (1997) *Proc. Natl. Acad. Sci. U.S.A. 94*, 3644−3649.
23. D'Souza, S. E., Ginsberg, M. H., Burke, T. A., Lam, S. C.-T., and Plow, E. F. (1988) *Science 242*, 91−93.
24. Smith, J. W., and Cheresh, D. A. (1988) *J. Biol. Chem. 263*, 18726−18731.
25. Calvete, J. J., McLane, M. A., Stewart, G. J., and Niewiarowski, S. (1994) *Biochem. Biophys. Res. Commun. 202*, 135−140.
26. Chen, L. L., Lobb, R. R., Cuervo, J. H., Lin, K.-C., Adams, S. P., and Pepinsky, R. B. (1998) *Biochemistry 37*, 8745−8755.
27. Taylor, M. F., Bhatacharyya, A. K., Rajagopalan, K., Hiipakka, R., Liao, S., and Collins, D. C. (1996) *Steroids 61*, 323−331.
28. Macdonald, S. G., Dumas, J. J., and Boyd, N. D. (1996) *Biochemistry 35*, 2909−2916.
29. Wilson, C. J., Husain, S. S., Stimson, E. R., Dangott, L. J., Miller, K. W., and Maggio, J. E. (1997) *Biochemistry 36*, 4542−4551.
30. Bisello, A., Mierke, D. F., Pellegrini, M., Rosenblatt, M., Suva, L. J., and Chorev, M. (1998) *J. Biol. Chem. 273*, 22498−22505.
31. Mannstadt, M., Luck, M. D., Gardella, T. J., and Jüppner, H. (1998) *J. Biol. Chem. 273*, 16890−16896.
32. Ploug, M., Ostergaard, S., Hansen, L. B., Holm, A., and Dano, K. (1998) *Biochemistry 37*, 3612−3622.
33. Bernier, S. G., Bellemare, J. M. L., Escher, E., and Guillemette, G. (1998) *Biochemistry 37*, 4280−4287.
34. Dormán, G., and Prestwich, G. D. (1994) *Biochemistry 33*, 5661−5673.
35. Kotzyba-Hibert, F., Kapfer, I., and Goeldner, M. (1995) *Angew. Chem., Int. Ed. 34*, 1296−1312.
36. Weber, P. J., and Beck-Sickinger, A. G. (1997) *J. Pept. Res. 49*, 375−383.

37. Greenberg, Z., Stoch, S. A., Traianedes, K., Teng, H., Suva, L. J., Rosenblatt, M., and Chorev, M. (1999) *Anal. Biochem. 266*, 153−164.

38. Fitzgerald, L. A., Steiner, B., Rall, S. C., Jr., Lo, S. S., and Phillips, D. R. (1987) *J. Biol. Chem. 262*, 3936−3937.

39. Calvete, J. J. (1995) *Proc. Soc. Exp. Biol. Med.*, 346−360.

40. Calvete, J. J., Arias, J., Alvarez, M. V., Lopez, M. M., Henschen, A., and Gonzalez-Rodriguez, J. (1991) *Biochem. J. 274*, 457−463.

41. Andrieux, A., Rabiet, M. J., Chapel, A., Concord, E., and Marguerie, G. (1991) *J. Biol. Chem. 266*, 14202−14207.